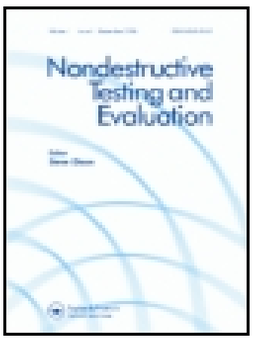

Nondestructive Testing and Evaluation

ISSN: 1058-9759 (Print) 1477-2671 (Online) Journal homepage: http://www.tandfonline.com/loi/gnte20

Effectiveness of phased array focused ultrasound and active infrared thermography methods as a nondestructive testing of Ni-WC coating adhesion

R. Rachidi, B. Elkihel, F. Delaunois & D. Deschuyteneer

To cite this article: R. Rachidi, B. Elkihel, F. Delaunois & D. Deschuyteneer (2019): Effectiveness of phased array focused ultrasound and active infrared thermography methods as a nondestructive testing of Ni-WC coating adhesion, Nondestructive Testing and Evaluation, DOI: 10.1080/10589759.2019.1566905

To link to this article: https://doi.org/10.1080/10589759.2019.1566905

Published online: 15 Jan 2019.

NONDESTRUCTIVE TESTING AND EVALUATION
https://doi.org/10.1080/10589759.2019.1566905

Taylor & Francis
Taylor & Francis Group

Effectiveness of phased array focused ultrasound and active infrared thermography methods as a nondestructive testing of Ni-WC coating adhesion

R. Rachidi[a], B. Elkihel[a], F. Delaunois[b] and D. Deschuyteneer[c]

[a]Department of Industrial Engineering, Maintenance & Mechanical Production, National School of Applied Sciences, Mohamed Premier University, Oujda, Morocco; [b]Metallurgy Unit, Faculty of Engineering, Mons University, Mons, Belgium; [c]Research and Industrial Support Department, Belgian Ceramic Research Centre, Mons, Belgium

ABSTRACT

The substrate/coating adhesion is a crucial parameter conditioning the quality of coating and its durability in service. For this reason, an inspection of the coating integrity, in particular, the presence of adhesion defects will be of great importance. The adhesion inspection is usually ensured by destructive methods, such as traction, interfacial indentation, four-point bending, testing scratch, etc. However, it is currently hampered by the absence of a satisfactory non-destructive method. Among the non-destructive testing technologies widely used in the industrial field, there are X-ray diffraction, ultrasonic inspection, and infrared thermography. In this paper, two methods are investigated: ultrasonic inspection, which becoming more efficient, especially with the emergence of phased array systems that allow to investigate different inspection angles and focusing depths, and the active infrared thermography. Experiments were performed on metallic coatings deposited on a mild steel substrate. Coatings were containing artificial defects (flat bottom holes with different diameters) at the interface and others were exempts of defects. Longitudinal waves with specific delay laws were generated through a phased array contact transducer (5 MHz of central frequency). Experimental results show that the ultrasonic method allows detecting and sizing defects with a diameter of 1 mm located in thick coatings.

ARTICLE HISTORY
Received 5 September 2018
Accepted 6 January 2019

KEYWORDS
Substrate/coating adhesion; nondestructive testing; phased array; coating; defects; detection

1. Introduction

Adhesion is quantified as the tensile strength of an interface between coating and substrate for a coated sample. This parameter is relatively low in the case of coatings produced by flame thermal spray in comparison with other techniques such as high-velocity oxy-fuel and laser cladding techniques [1,2]. In this process, the coating is mechanically bonded to the substrate [3,4]. Several authors [5–7] have reported that substrate/deposit adhesion is the most searched property especially for coatings operating under severe thermal and/or mechanical conditions, where they sometimes tend to peel off during operation. However, an accurate testing is very important. The inspection of adhesion is usually ensured by destructive methods; generally increasing mechanical action is applied until the coating is separated from the substrate.

CONTACT R. Rachidi r.rachidi@ump.ac.ma

Although the assessment of the state of test object using destructive testing is usually more reliable, the destruction of this object generally makes this type of testing more costly the non-destructive testing. A number of destructive testing methods have been developed to evaluate adhesion and delamination toughness of thermal spray coatings and for other techniques, and are described in several literature works [1,2,8–11]. However, no method meets all requirements. Among the non-destructive testing methods, those using ultrasonic transducers and infrared thermography are interesting in view of the fact that the number of applications in industrial field increases. These methods are used to get accurate information about the physical integrity of metal parts and can be used to inspect a coating-substrate system.

Ultrasonic inspection is a non-destructive method in which beams of high-frequency sound waves are introduced into materials for the detection of surface and subsurface flaws. Discontinuities like cracks, disbonds, pores, inclusions are detected by causing partial reflection of the ultrasonic waves. The reflected beam is displayed and then analysed to define the presence and location of flaws or discontinuities [12]. The fastest means of scanning is the use of an array of transducers that are scanned electronically by triggering each of the transducers sequentially. Infrared thermography inspection is a non-destructive method widely used in industries for non-destructive testing of materials [13–16]. This method consists of measuring infrared heat radiation at the surface, used to detect spatial variations in the temperature of the piece surface to be inspected. The analysis reveals defects by looking for abnormal hot spots after thermal excitation. The purpose of this paper is to evaluate the performance and limitations of the focused ultrasonic method and the active infrared thermography, in terms of detection, positioning and sizing of adhesion defects at the coating-substrate interface. A phased array transducer is used for the ultrasonic inspection and a thermal camera for the thermography inspection. These two methods, despite their many inspection advantages, are currently not used for thick thermal spray coatings. This work represents a new and relevant aspect of the application. The experiments are carried out on Ni-WC. The results are represented with A-scan signals, S-scan and B-scan ultrasonic imaging.

2. Materials and methods

2.1. Non-destructive testing by ultrasonic waves

2.1.1. Phased array transducers

Phases Array ultrasonic method that is used in the medical field to test the human body, have often been adapted in industrial field for materials inspection. The principle of this method is based on the use of a transducer consisting of an electronic array containing a dozen piezoelectric elements, which have a parallelepiped shape and are joined to each other. The excitation of these crystals takes place in two ways: either to excite all of them at the same time, which will allow to have a narrow beam, or to excite them by subgroups (apertures) where a number of crystals will be excited at the same time.

Phased array transducers have certain advantages. Compared to planar transducers, they allow better axial and lateral resolution and better sensitivity to discontinuities, which permit the detection of very small defects and very close defects. Compared to all transducers including other types of focused transducers, they allow the possibility of focusing at different depths and angles. They also allow the possibility that the focusing in transmission is different from that in reception by modifying the laws of delays.

2.1.2. Ultrasonic inspection of coating adhesion

It is actually very difficult to produce a coating that has no risk of delamination and discontinuities. During the coating process, discontinuities such as voids, cracks, inclusions or corrosion can be shown up inside the coating or even delamination at the interface by lack of adhesion. For that reason, testing during use periodically is often essential. Figure 1 shows a diagram on how ultrasonic waves propagate in thermal spray coating, (a) a coating adhering to the substrate, (b) a less adherent coating and (c) a detached coating of the substrate (poor coating). The bottom echo has a large amplitude in the case (a). This amplitude decreases with the integrity of the coating. In the case of poor adhesion, the bottom echo is highly decreased and even may not be detected, because the ultrasonic waves attenuate strongly in the presence of air (lack of adhesion) and therefore they cannot continue its way to the bottom of the substrate. Indeed, the integrity of the coating close to the substrate can be evaluated by detecting precisely the bottom echo [17]. If the inspection is done on the substrate side and surface irregularities are present at the surface of the coating, the bottom echo decreases more in comparison with the case of a smooth surface, since most of the ultrasonic waves are reflected in the directions of the irregularities. In the present study, the relationship of non-linearity of the ultrasonic response for the coating-substrate interface is exploited to deduce the adhesion.

2.2. Non-destructive testing by infrared thermography

2.2.1. Thermal camera

Thermal cameras are devices for measuring infrared radiation and thus the temperature of objects. The radiometric system converts the power of the radiation into digital or analogue signals that are transcribed into temperature. The infrared camera allows two-dimensional

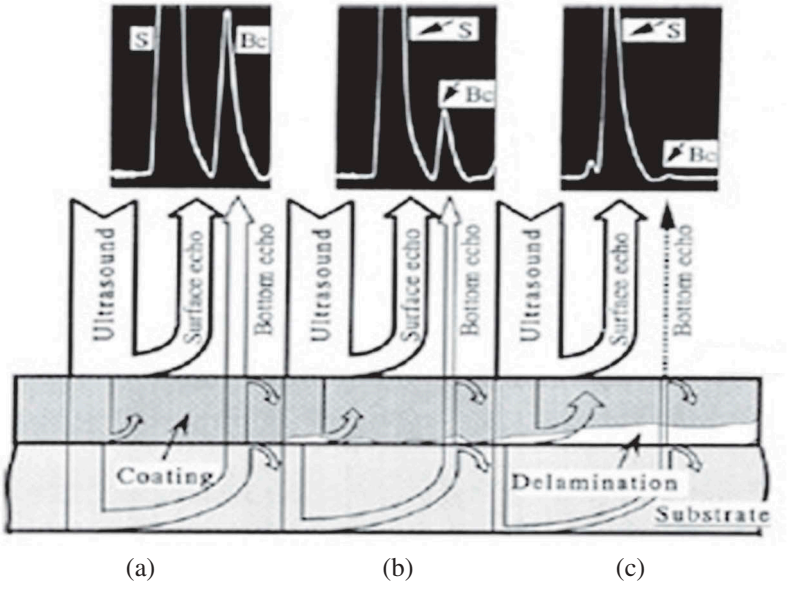

Figure 1. Influence of the coating integrity on the reflection and transmission of ultrasonic waves. The ultrasonic response is indicated as echoes [17].

measurement of the temperature without contact, in real-time and can be used in several ranges of temperature according to the emissivity of the surface. The thermal image captured by the camera and termed a thermogram consists of pixels juxtaposed next to each other, and each pixel is assigned more or less intense shade of grey depending on the temperature degree.

2.2.2. Parameters affecting infrared thermography

The accuracy in the temperature of material estimated by the thermal camera is often closely related to the accuracy in the assessment of the input parameters. Indeed, the main parameters that must be provided to the camera are: the emissivity of the inspected material, the reflected apparent temperature, the distance between the material and the camera, the relative humidity and the environment temperature. The accuracy of these input parameters becomes less critical if the inspected material has a high emissivity and is significantly warmer than its environment. Similarly, these mentioned parameters may be neglected if the aim is to perform qualitative diagnosis such as defects detection in the case of metal coatings.

2.2.3. Active infrared thermography

Dynamic or active analysis consists of heating the surface of the inspected material by means of an external source such as flash lamps, heat lamps, ultrasonic energy, and measuring the resulting temperature rise with an infrared camera. Active infrared thermography is one of the non-destructive testing methods widely used to detect defects in metallic and composite materials and structures, and it is more suitable for defects located near the surface on which the inspection is performed. The presence of defects, cracks, for example, which are an obstacle to the propagation of heat by conduction, are manifested locally on the thermal images by an abnormally slow return to ambient temperature. The active infrared thermography can be in reflection mode or in transmission mode.

3. Materials and experimental procedure

The material used for inspection is S235JR mild steel substrate with 10 mm thickness, on which is deposited a layer of Ni-WC with a thickness of 1.3 mm. As-sprayed and rectified Ni-WC coatings are investigated (Figure 2). The rectified coating has an average surface roughness of 0.24 μm. These coatings were made by laser cladding technique in the Belgian Ceramic Research Centre at Mons-Belgium.

The sample is prepared as shown in Figure 3. The artificial defects studied are flat bottom holes drilled on the uncoated face of the steel substrate with different diameters and at different depths. Their diameters ‘d’ are, respectively, 1 mm, 2 mm, and 4.1 mm. The depth ‘x’ at which each hole is located is 9 mm and 10 mm for the 1 mm diameter, 8 mm and 10 mm for the 2 mm and 4.1 mm diameters.

The test stands shown below were assembled at the PFT2M technological platform of Industrial Engineering department at the National School of Applied Sciences-Oujda. Ultrasonic inspection was carried out using OLYMPUS Omniscan SX system (Figure 4), with phased array transducer of 32 active elements (the distance separating two successive active elements is 0.6 mm), 22 mm in diameter and central frequency of 5 MHz, placed

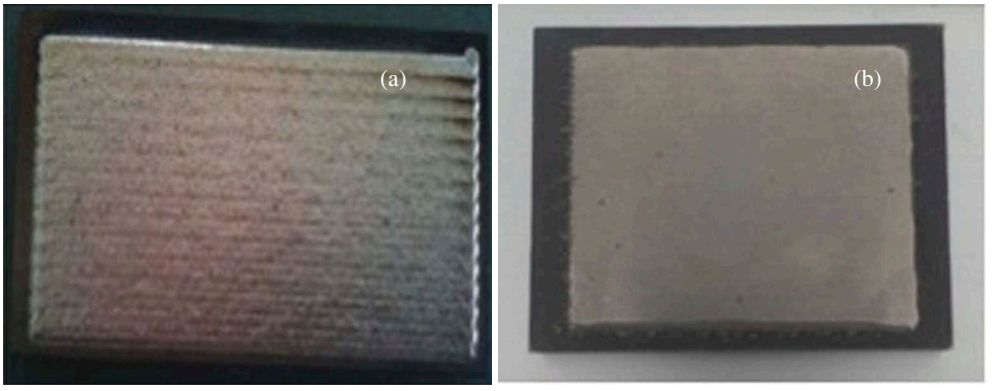

Figure 2. Laser cladded coating. (a) as-sprayed, (b) rectified.

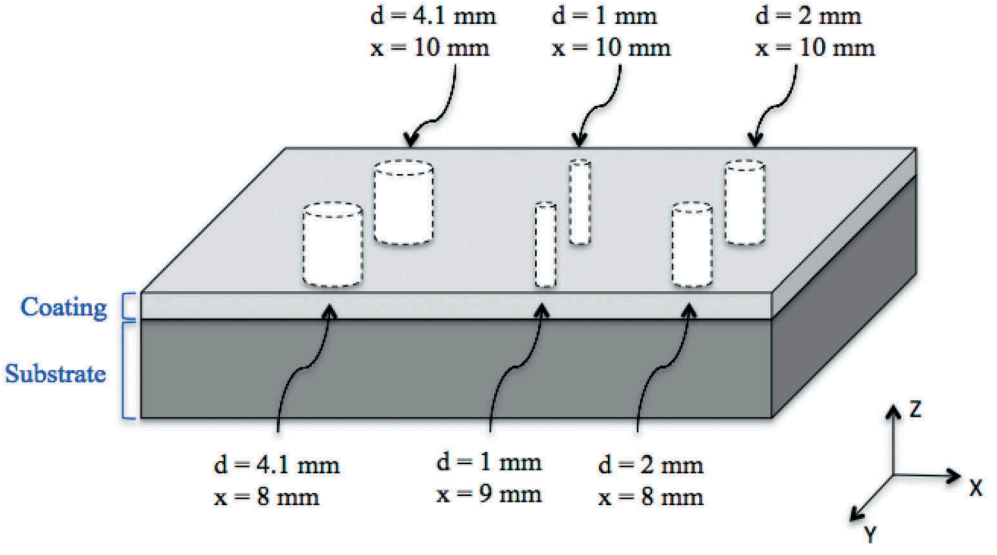

Figure 3. Representative schema of the studied defects.

on a 0° Plexiglas shoe with a height of 23 mm. This system allows to excite the transducer with adequate delays, to receive the signals and to put them in various displays, which can be easily exploited.

Figure 5 shows the set-up used for thermography tests using thermal stimulation by a lamp. It consists of a FLIR T440 infrared camera used to collect data. This device consists of an uncooled microbolometer detector of 320 × 240 pixels, sensitive in the infrared spectral band of 7.5–13 μm (far infrared). Some important characteristics of the FLIR T440 infrared camera are summarised in Table 1. Two lamps serving as heating means are positioned at about 1 m and oriented at an angle of 30° to the normal of the coating surface, in order to obtain the uniform distribution of heat flux on the surface. The infrared camera is positioned at a distance, which allows us to focus and take pictures of the entire sample. The obtained information is stored in a computer.

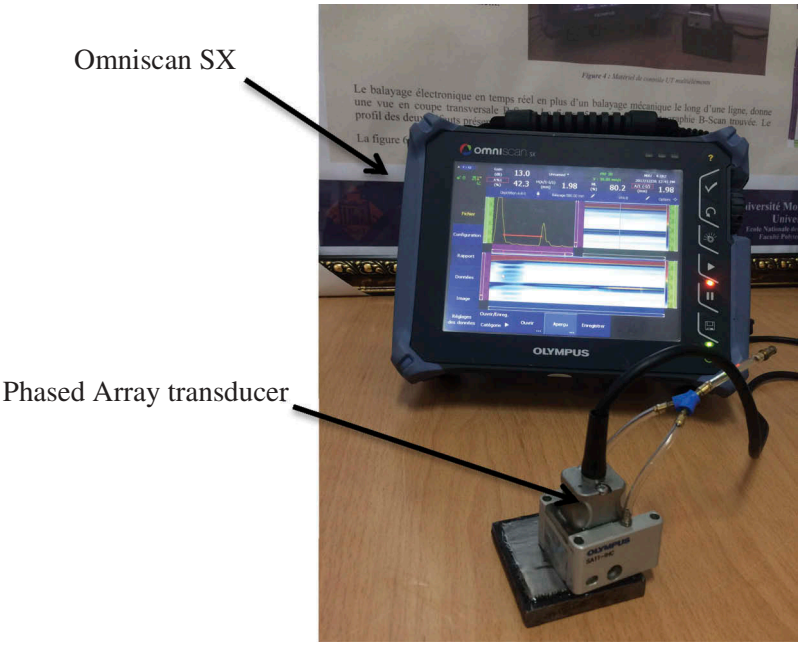

Figure 4. Equipment for ultrasonic testing.

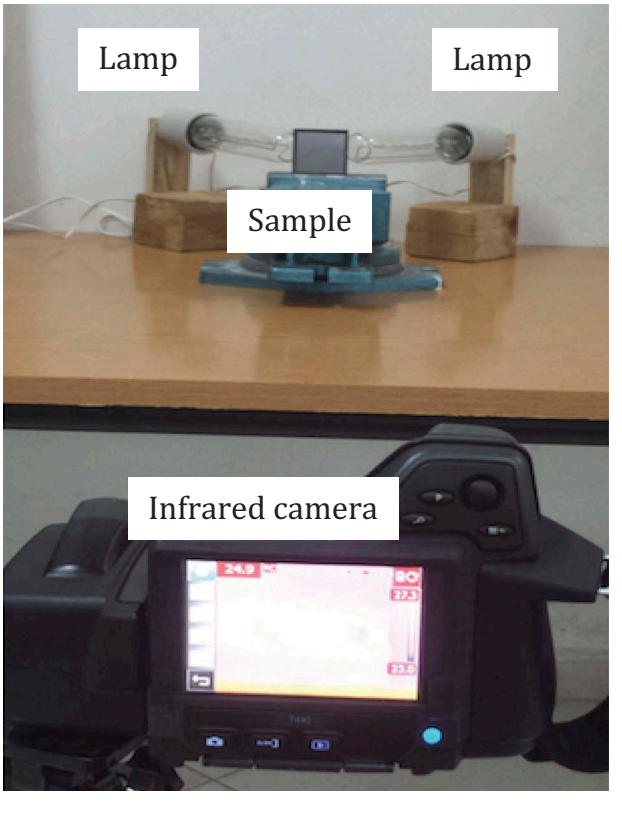

Figure 5. Experimental set-up of active infrared thermography.

Table 1. Infrared thermography parameters.

Parameters	
Temperature range	Min = −20°C to Max = 1200°C
Detector type	Uncooled microbolometer, 320 × 240 elements (76,800 pixels)
Minimum focusing distance	40 cm
Display frequency	60 Hz
Correction on the emissivity	Variable from 0.01 to 1 or selected from the list of materials
Spectral band	7.5–13 μm
Measurement accuracy	±2°C or ±2%

The experiment will consist of stimulating the surface of the substrate/coating system with lamp. Indeed, the tests are performed by means of both the one-side pulse process (the camera and the excitation source are on the coating side), which is a reflection control and two-sided control or transmission control (the camera is on the coating side while the excitation source is on the substrate side). This solicitation generates heat on the surface. The surface temperature rises and causes heat transfer phenomenon by conduction in the coated part. The temperature is measured on the coating surface by the infrared camera. Then, the thermograms obtained are recorded at regular intervals of time and visualised afterwards using appropriate software.

4. Results and discussion

4.1. Influence of surface condition on the inspection quality

As-sprayed and rectified coatings are used to obtain different bottom echoes. Therefore, attenuation is measured from the amplitude decrease of the successive bottom echoes. The obtained results are shown in Figure 6. Both coated samples are 11 mm thick and the working frequency is 5 MHz using the Beer–Lambert law:

$$A_2 = A_1 \exp(-\alpha x) \tag{1}$$

A_1 is the first bottom echo, A_2 is the second bottom echo, x is the thickness traversed by the wave (x= $2e$) and α is the attenuation coefficient. The attenuation coefficient is expressed as follows:

$$\alpha = \frac{1}{2e} \ln(A_1/A_2) \tag{2}$$

e is the thickness of the test piece (mm).

According to Figure 6, the attenuation coefficient in the case of as-sprayed coating is α = 0.035 dB.mm^{-1} (Figure 6(a)) against α = 0.014 dB.mm^{-1} for the rectified coating (Figure 6(b)). There is an exponential decrease in the echoes amplitude of the successive bottom. From these results, it can be concluded that the condition of the coating bottom influences the attenuation. Indeed, the attenuation increases with the surface roughness of the bottom.

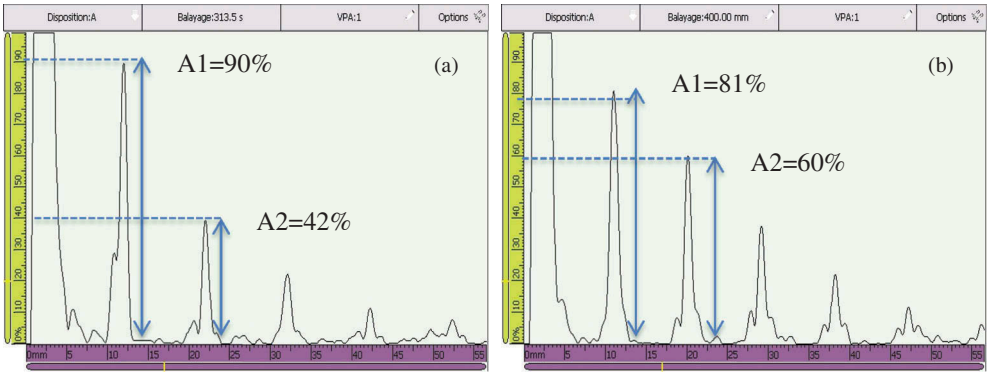

Figure 6. A-scan data of: (a) as-sprayed coating and (b) rectified coating.

4.2. Preliminary inspection of the uncoated and coated pieces

In this experiment, the ultrasonic beam is focused at d = 4 mm. The uncoated and coated pieces with the dimensions cited in the description part of the material are evaluated. Figure 7 shows the result of the ultrasonic inspection.

In Figure 7, A-scan is a display of signal amplitude versus time at a given transducer position. In the S-scan format, the echo's amplitude is coded in colours; the more the colour tends towards the red, the greater the amplitude is.

For the uncoated piece (Figure 7(a)), it can be seen that the echoes have high amplitude, which does not attenuate rapidly. The echo's amplitude is still high after the sixth bottom reflection, marked by the red colour. This response seems logical since the wave when it arrives at the piece bottom, it encounters the interface separating the piece from the air and since the ultrasonic waves do not propagate in the air, the wave is totally reflected. Therefore, the wave's amplitude is maximal. Figure 7(b) represents the result of the control for the coated piece. It can be seen that the wave attenuates rapidly, which is represented by the yellow colour after the third bottom reflection and low amplitude after the fifth bottom reflection. This can be justified by the presence of an interface between the two materials (coating-substrate interface) whose impedances are close. In this case, almost the entire wave passes in the coating. Since the coating surface is rough, the wave is diffused on the surface asperities. Then, the wave is die out in the asperities and low energy could return to the transducer. This explains the fact that the wave has attenuated rapidly. Furthermore, it is important to note the absence of the interface echo except for few traces just above the bottom echo. This finding leads us to conclude that the interface echo is merged with the bottom echo due to the low coating thickness, which is of 1 mm. The echoes are very straight which leads us to conclude that the adhesion between the coating and the substrate is good.

4.3. Simulation of the influence of excited elements number

It is important to note that the thickness of the coating is 1 mm, and the inspection was carried out on the substrate side. Tests are carried out using 0° longitudinal waves. A linear electronic scan is applied by sequences of eight elements displaced along the array with one-element increments and no field focusing was applied.

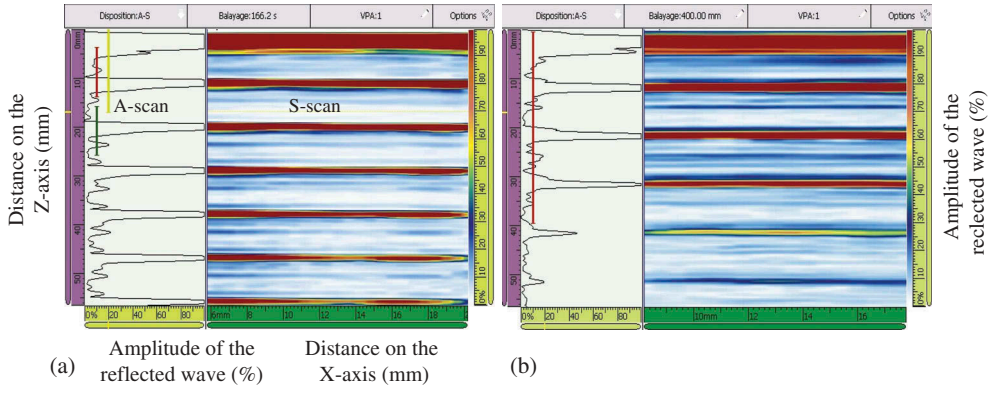

Figure 7. Visualisation of the obtained signals in A-scan and S-scan formats. (a) Uncoated piece, (b) coated piece.

According to Figure 8(a), the first echo represents the excitation or surface echo. The second echo is the bottom echo (first bottom reflection inside the examined sample) while the other echoes are bottom reflections. The displayed echoes appear fluctuated. In the first interpretation, this may be due to the beam profile sent to the sample, which is depending on the transducer diameter, i.e. the number of exited elements. The ultrasonic field radiated inside the sample by the phased array transducer is then simulated using appropriate software. This software is dedicated to the visualisation of the acoustic field in metallic parts. Figure 9 shows the results of the simulation as a function of the exited elements number.

The results show that as the diameter increases, the focal zone becomes narrow, then the resolution becomes better and the signal-to-noise ratio increases; then, the field fluctuations decrease considerably. In addition, as the diameter increases, the focal zone moves in depth, i.e. the distance from the near field increases. Theoretically, for a good spatial resolution, it will be necessary to use the maximum number of excited elements. The case of 16 excited elements has the narrower field contrary to the case of 8 and 4 excited elements. Then, for better inspection of the sample, an aperture of 16 elements will be the right choice in this study. Figure 8(b) shows the inspection of the coating with the excitation of 16 elements where an improvement in the echo's quality is observed.

4.4. *Influence of coating thickness*

Non-destructive testing by focused ultrasonic beam using phased array transducer of the adhesion for three different coating thicknesses was performed. This study aims to analyse the effect of the coating thickness on the propagation of ultrasonic waves and thus the ability to detect defects at the interface. The working frequency was 5 MHz, the focusing depth was d = 9 mm and the number of excited elements was 16. Some characteristics of the coatings being inspected are mentioned in Table 2. The ultrasonic inspection was carried out on the substrate side in transmission-reception mode. The results obtained for each layer are shown in Figure 10.

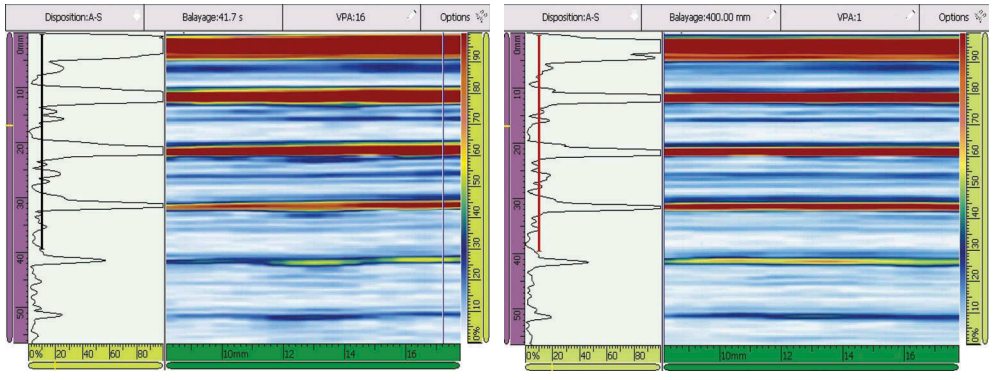

Figure 8. Visualisation of the obtained signals in A-scan and S-scan formats. (a) using 8 excited elements, (b) using 16 excited elements.

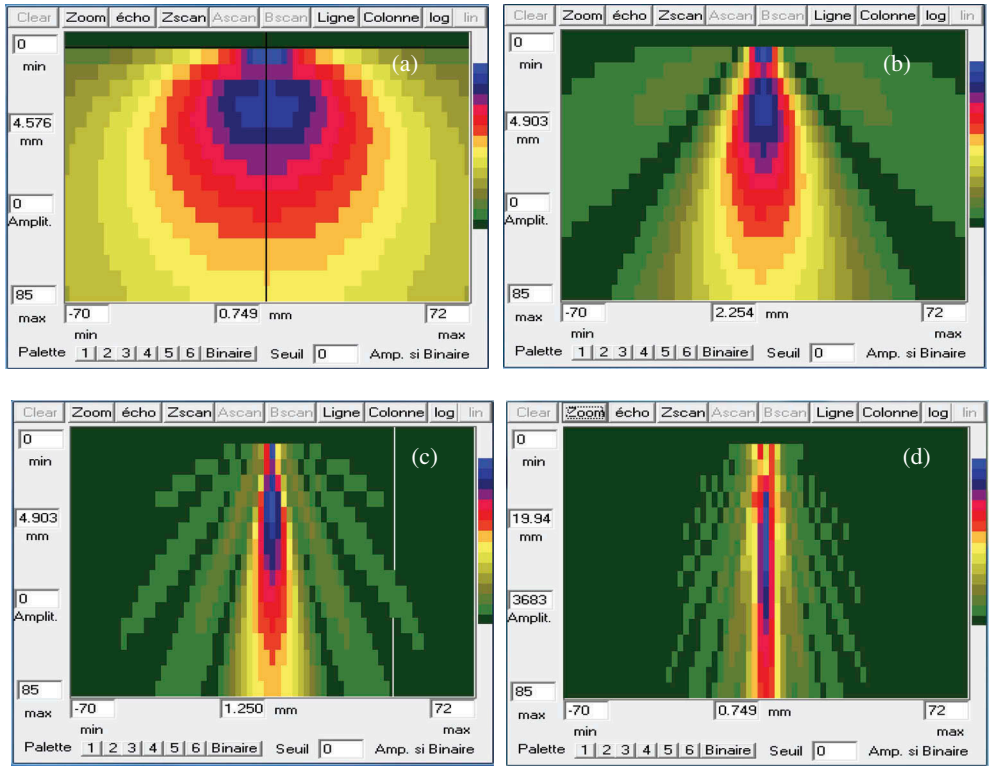

Figure 9. Mapping of the acoustic field radiated by phased array transducer. (a) 1 element, (b) 4 elements, (c) 8 elements and (d) 16 elements.

By analysing the results and identifying each echo on the A-scan/S-scan format, the distances travelled by the ultrasonic wave and corresponding to the different echoes are measured using the Omniscan SX ultrasonic system. These measurements are in agreement with the theoretical calculation of distance with a bit difference. This lag can be explained by

Table 2. Data of the different coatings.

Coating	Substrate thickness (mm)	Coating thickness (e) (mm)
Ni-WC	10	1.7
Ni-WC	10	1.3
Ni-WC	9.3	4.5

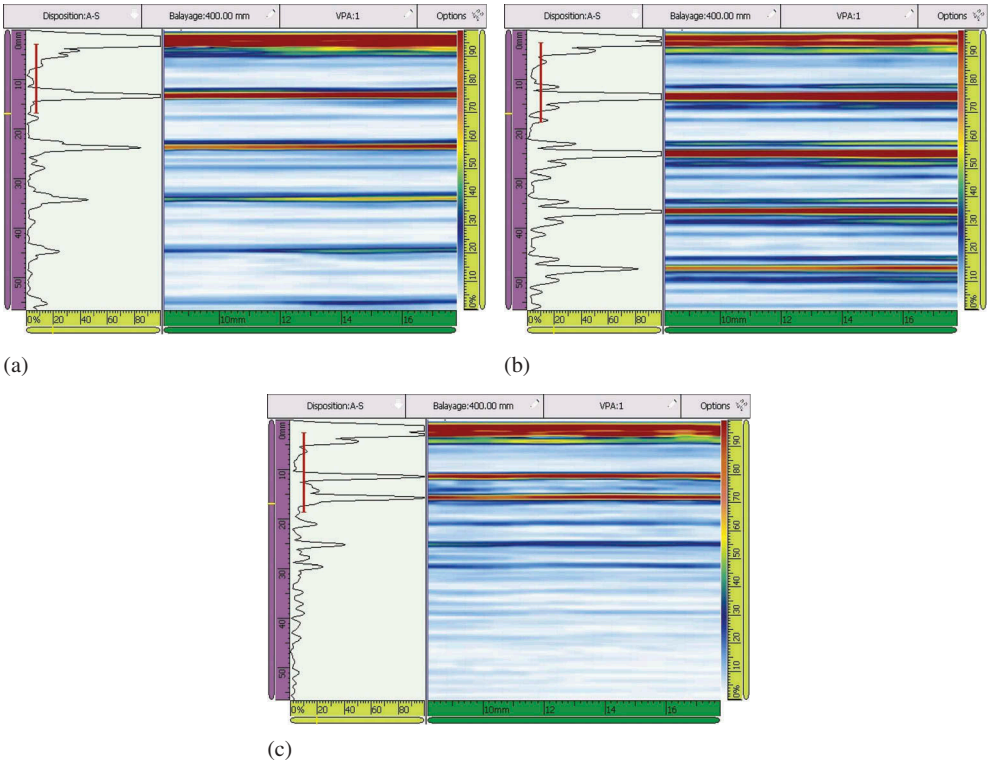

Figure 10. A-scan and S-scan mapping of coated pieces vs. thickness: (a) e = 1.3 mm,(b) e = 1.7 mm, (c) e = 4.5 mm.

the difference in propagation velocity between the substrate (mild steel) and the coating layer (composite). Indeed, it has been considered that the inspected material is made of steel only, while the ultrasonic wave actually crosses two materials of different physical properties. According to the interface echoes, the three coating layers appear to be well adherent to their substrates, which is in agreement with the microscopic observation of the interface of the laser cladded deposits. For coatings with small thickness e = 1.3 mm, the echoes corresponding to the interface are almost confused with those of the piece bottom, which makes difficult the detection of the adhesion defects with the parameters used in this experiment.

4.5. Influence of focusing depth

The ultrasonic inspection was carried out with the parameters presented in the previous Section 4.4. The parameter that has been changed in this study is the focusing depth d. The

number 1 is used to designate the coating thickness e = 1.3 mm, the number 2 for the coating of e = 1.7 mm thickness and the number 3 for the coating thickness e = 4.5 mm. The results obtained for each coating are shown in Figure 11.

For the three layers, the comparison of A-scan/S-scan versus focusing depth is made. The results show that the focusing at the interface gives the best results.

4.6. Ultrasonic inspection of piece with artificial defects using array transducer

Figure 12(a–c) shows the A-scan, S-scan and B-scan data formats for the three defects with the depth d = 10 mm. Similar results are obtained for the three defects with the depth d = 9 mm, that is why they are not presented in this manuscript. During the inspection, the ultrasonic system shows three indications: the initial pulse, a second echo superposed to the first, which corresponds to the interface (due to the difference in acoustic impedance of the coating material and steel), and a third echo corresponding to the reflection on the bottom; the second surface of the substrate. The defects of different diameters 1 mm, 2 mm and 4.1 mm are clearly detected by the ultrasonic inspection.

The region where the bonding between the coating and the substrate is supposed to be acceptable is where the echo of the interface is minimal. When the echo of the interface increases, the bonding becomes questionable. When there is no return of the bottom echo, it can be assumed that there is delamination and when there is no return of the interface echo, it can be assumed that there is no interface and that the material is unique. The presence of a defect in the present study is indicated on the S-scan and B-scan by the discontinuity of the

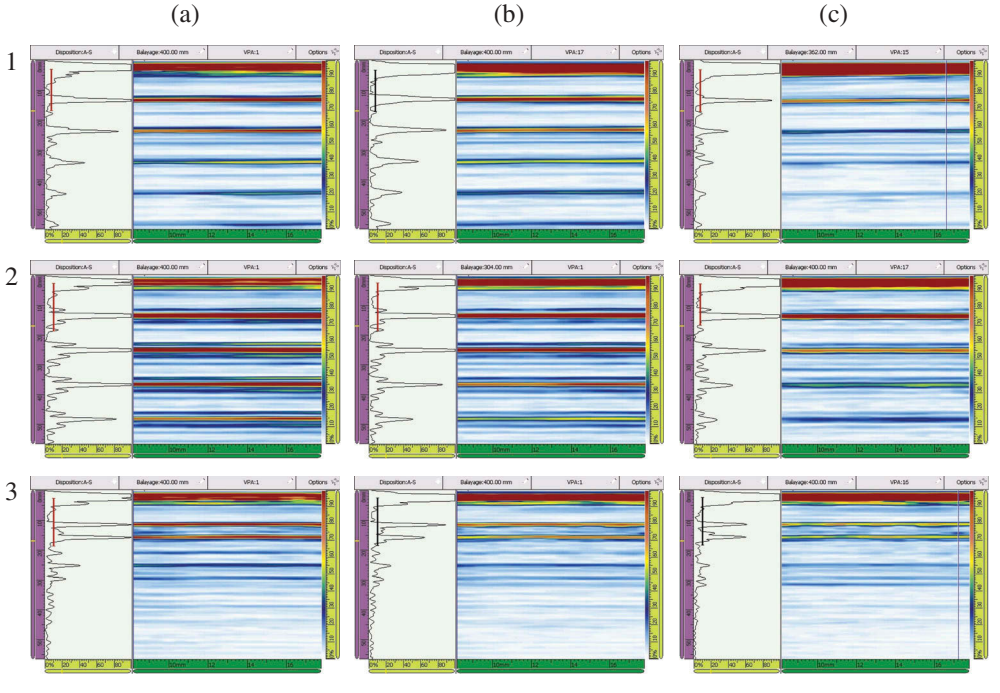

Figure 11. A-scan and S-scan mapping of coated pieces vs. focusing depth: (a) d = 9 mm,(b) d = 5 mm, (c) d = 2 mm.

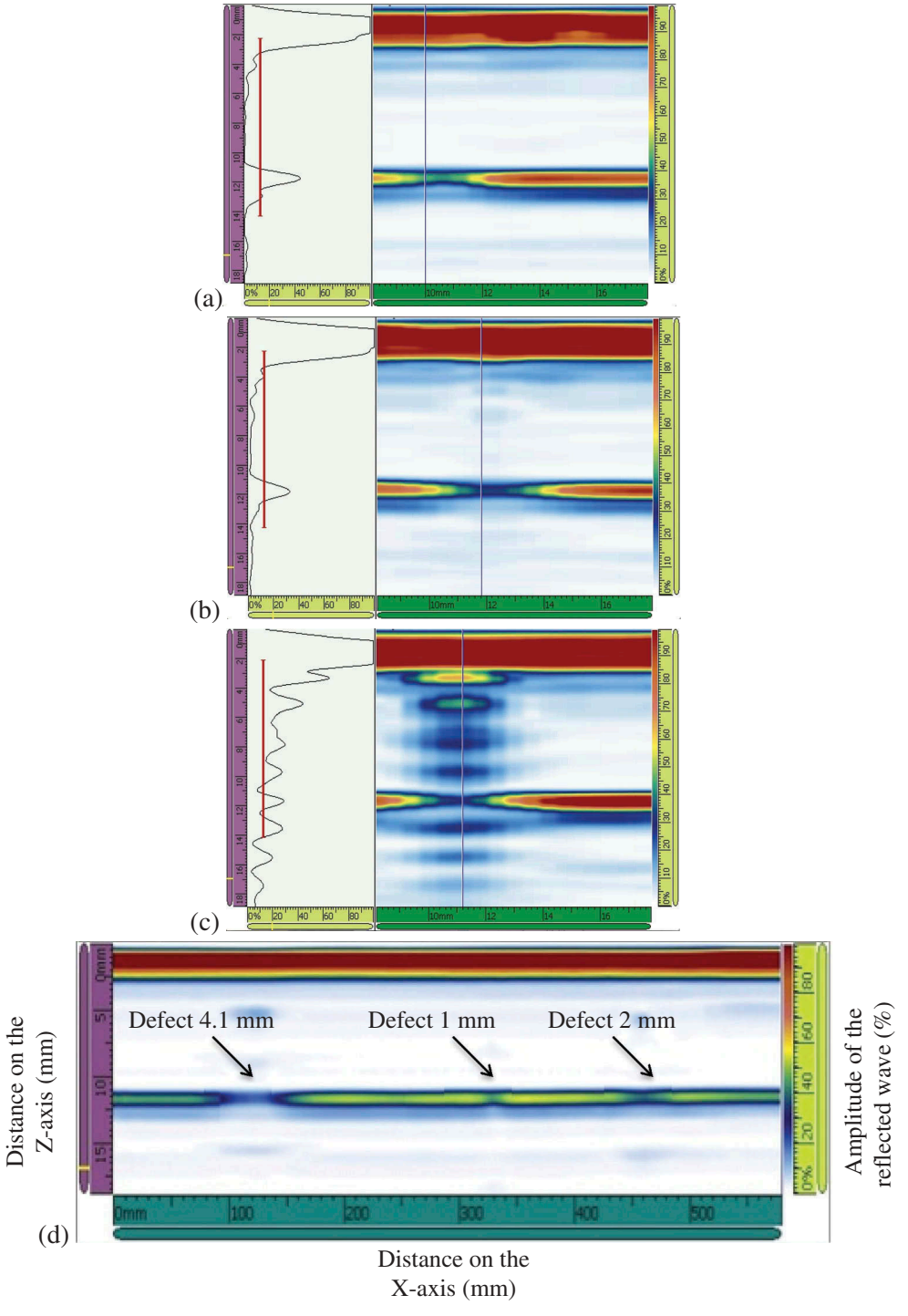

Figure 12. A-scan/S-scan formats for artificial defects. (a) d = 1 mm, (b) d = 2 mm, (c) d = 4.1 mm, (d) B-scan mapping.

bottom echo. This discontinuity is becoming wider as the defect diameter increases from 1 mm to 4.1 mm. It is the defects of diameter 2 mm and 4.1 mm that appear better.

4.7. Inspection of piece with artificial defects using active infrared thermography

The coating had been overlaying with a thin layer of black paint to produce a reasonably uniform emissivity. In the infrared thermography test, a sequence of 120 thermograms was recorded for duration of 1 h. The tests were conducted using the one-sided inspection (the camera and stimulation source are on the same side of the sample; the coating surface) and the two-sided inspection (the camera and stimulation source are located on opposite sides of the sample). Figure 13 shows the thermograms obtained from the two-sided inspection, which proved to be the right choice in terms of efficiency and manipulation for the selected sample. According to the results, no trace of defects was detected even for the large diameter defect. Basically, the defects should appear as dark traces because the heat at these locations is poorly conducted and therefore, the temperature is minimal.

The same test was reproduced by modifying the heat source; replacing the lamps by a flame whose temperature exceeds 1200°C. The surface temperature of the coating rises to 400°C approximately. As shown in Figure 14 taken after 15 min of heating, the defects located at the interface are not detectable by the camera. The conclusion that can be made is this method has proven to be less effective in detecting defects in such coatings at least for the parameters used in this experiment. One explanation could be the thickness of the test piece; as the test piece thickness increases, thermal inspection becomes less effective because the possible depth of the defect may be greater [17].

5. Conclusion

Nowadays, coating for protection against wear and corrosion are massively used in a large number of industrial applications. Thus, it will be of great importance to characterise their integrity during service depending on the working conditions. In this work, two very popular methods in the field of non-destructive testing are used, in

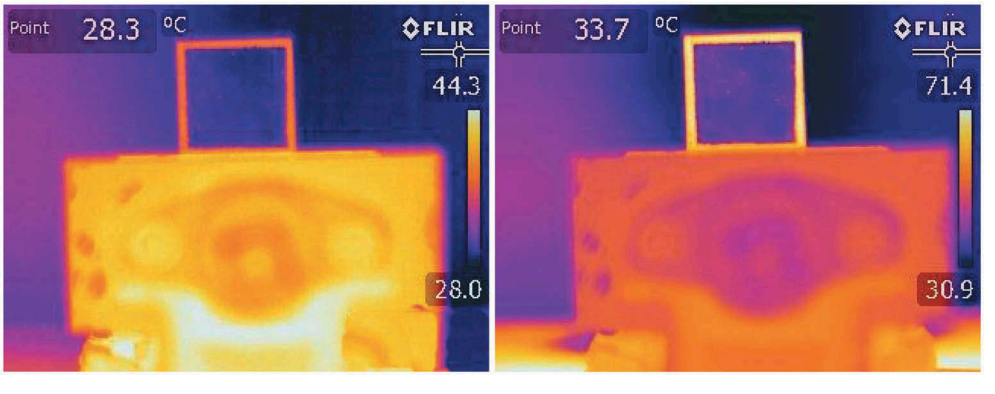

Figure 13. Thermogramms of the piece with artificial defects. After 10 min of heating (left), after 1 h of heating (right).

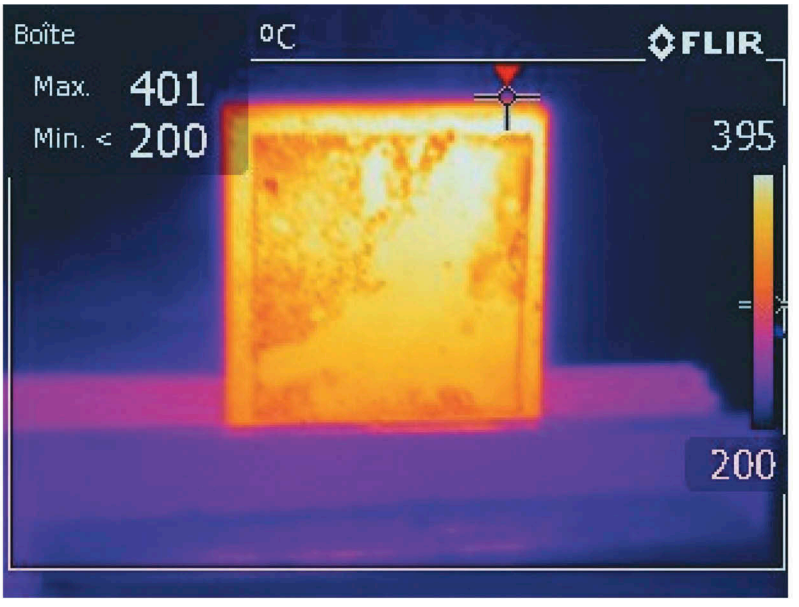

Figure 14. Thermogramm using a flame as heat source.

order to compare their effectiveness in detecting defects that may occur at the interface of thick metal coatings. The results obtained by the focusing ultrasonic method using a phased array transducer and the active infrared thermography methods are compared. The thermograms show no thermal trace of the defects, whereas the A-scan, S-scan and B-scan formats show clearly the six defects on the inspected sample. These results allow to conclude that Infrared thermography method does not permit the detection of adhesion defects in thick coatings, unlike the ultrasonic method which was shown to be an efficient method for the detection, positioning and also dimensioning of this type of defects.

Acknowledgments

The authors wish to thank Professor Elamrani Mostafa from Faculty of Sciences-Oujda (Morocco).

Disclosure statement

No potential conflict of interest was reported by the authors.

Funding

This work was supported by the CNRST (Morocco) and the ARES-CCD development cooperation (Belgium); Centre National pour la Recherche Scientifique et Technique;

References

[1] Thiem PG, Chornyi A, Smirnov IV, et al. Comparison of microstructure and adhesion strength of plasma, flame and high velocity oxy-fuel sprayed coatings from an iron aluminide powder. J Surf Coat Technol. 2017;324:498–508.

[2] Anders H, Anders N. Adhesion testing of thermally sprayed and laser deposited coatings. J Surf Coat Technol. 2004;184:208–218.

[3] Lu SP, Kwon OY. Microstructure and bonding strength of WC reinforced Ni-base alloy brazed composite coating. J Surf Coat Technol. 2002;153:40–48.

[4] Bergant Z, Grum J. Quality Improvement of flame sprayed, heat treated, and remelted NiCrBSi coatings. J Therm Spray Technol. 2009;18:380–391.

[5] Danlos Y, Costil S, Liao H, et al. Influence of Ti-6Al-4V and Al 2017 substrate morphology on Ni-Al coating adhesion-Impacts of laser treatments. J Surf Coat Technol. 2011;205:2702–2708.

[6] Aleksandar V, Saioa A, Gregory F, et al. Evaluation of adhesion/cohesion bond strength of the thick plasma spray coatings by scratch testing on coatings cross-sections. Tribol Int. 2011;44:1281–1288.

[7] Wang X, Wang C, Atkinson A. Interface fracture toughness in thermal barrier coatings by cross-sectional indentation. Acta Mater. 2012;60:6152–6163.

[8] Arash G, Sanjay S, Kenneth H, et al. Damage mechanisms and cracking behavior of thermal sprayed WC-CoCr coating under scratch testing. Wear. 2014;313:97–105.

[9] Marcano Z, Lesage J, Chicot D, et al. Microstructure and adhesion of Cr_3C_2-NiCr vacuum plasma sprayed coatings. J Surf Coat Technol. 2008;202:4406–4410.

[10] Sexsmith M, Troczynski T. Peel adhesion test for thermal spray coatings. J Therm Spray Technol. 1994;3:404–411.

[11] Yu HL, Zhang W, Wang HM, et al. Comparison of surface and cross-sectional micro-nano mechanical properties of flame sprayed NiCrBSi coating. J Alloy Compd. 2016;672:137–146.

[12] ASM International Metals Handbook Ninth Edition. Nondestructive evaluation and quality control. Vol. 17. Metals Park, Ohio: ASM International.Year of publication; 1989.

[13] Schroeder JA, Ahmed T, Chaudhry B, et al. Non-destructive testing of structural composites and adhesively bonded composite joints: pulsed thermography. Composites. 2002;33:1511–1517.

[14] Tashan J, Al-Mahaidi R. Detection of cracks in concrete strengthened with CFRP systems using infra-red thermography. Composites. 2014;64:116–125.

[15] Senni L, Ricci M, Palazzi A, et al. On-line automatic detection of foreign bodies in biscuits by infrared thermography and image processing. J Food Eng. 2014;128:146–156.

[16] Gaudenzi P, Bernabei M, Dati E, et al. On the evaluation of impact damage on composite materials by comparing different NDI techniques. Compos Struct. 2014;118:257–266.

[17] Lian D, Suga Y, Shou G, et al. An ultrasonic testing method for detecting delamination of sprayed ceramic coating. J Therm Spray Technol. 1996;5:128–133.